Ultrabroadband 50-130 THz pulses generated via phase-matched difference frequency mixing in $LiIO_3$

Thomas Zentgraf, Rupert Huber*, Nils C. Nielsen, Daniel S. Chemla, and Robert A. Kaindl

Department of Physics, University of California at Berkeley, and Materials Sciences Division,
E. O. Lawrence Berkeley National Laboratory, Berkeley, California 94720, USA

We report the generation of ultrabroadband pulses spanning the 50-130 THz frequency range via phase-matched difference frequency mixing within the broad spectrum of sub-10 fs pulses in $LiIO_3$. Model calculations reproduce the octave-spanning spectra and predict few-cycle THz pulse durations less than 20 fs. The applicability of this scheme is demonstrated with 9-fs pulses from a Ti:sapphire oscillator and with 7-fs amplified pulses from a hollow fiber compressor as pump sources.

OCIS codes: 160.4330, 190.2620, 320.7110

Ultrafast mid-infrared (mid-IR) and ultrabroadband terahertz (THz) spectroscopy has evolved into a powerful tool in chemistry and materials science. Femtosecond pulses in this range can probe e.g. molecular vibrational dynamics, electronic gaps in superconductors, plasma quantum kinetics and intersubband transitions in semiconductors, or phonon coupling in semimetals.[1–5]

Mid-IR femtosecond pulses are often generated via intricate cascades of optical parametric amplification and difference frequency mixing stages.[6] While the latter provide high pulse energies, a significantly simpler route involves mixing the components within the broad spectrum of individual fs pulses (henceforth called visible pulses). This was demonstrated by optical rectification of Ti:sapphire oscillator pulses on various semiconductors.[7,8] Phase-matched difference frequency mixing within the broad spectrum of single 13-fs pulses was reported in GaSe,[9,10] providing mid-IR fs pulses tunable from 7–20 μm and a significant boost of IR power. Direct ultrabroadband electro-optic sampling of such few-cycle pulses revealed an inherent stability of the electric field profile.[11] This finding corresponds to a precisely locked carrier-envelope phase that results from difference frequency mixing within a single pulse spectrum.[12,13] Thin naturally-cleaved GaSe emitters were shown to generate

detectable frequency components spanning several octaves throughout the far- and mid-IR.[14,15] However, the center frequencies could not be tuned beyond 50 THz due to exceedingly large angles of incidence required in this phase-matching scheme. This motivates the search for new compact fs sources to cover all of the mid-IR.

In this Letter, we demonstrate a phase-matched source of ultrabroadband 50-130 THz pulses, generated in $LiIO_3$ via difference frequency mixing within broad visible pulse spectra. THz pulse energies and spectra are characterized for different sub-10 fs Ti:sapphire pump sources. We present calculations of the THz electric field and the phase-matching conditions for this nonlinear process. This constitutes a novel compact and broadband THz source around $\lambda \approx 3-7$ μm, resonant to important molecular vibrations and electronic excitations in solids.

In $LiIO_3$, difference frequency mixing can be phase-matched as a type-I nonlinear process with $\Delta\nu^{(o)} = \nu_2^{(eo)} - \nu_1^{(o)}$. Here, ν_1, ν_2 are frequencies of the visible pulse, $\Delta\nu$ is the THz difference frequency, while o and eo designate the ordinary and extraordinary polarizations. In the following, we investigate a 113-μm thick, free-standing $LiIO_3$ crystal cut at $\theta = 21.5°$ for phase-matching at normal incidence.

In a first set of experiments, a 78-MHz Ti:sapphire oscillator is used to deliver 9-fs pulses around 790 nm wavelength. The setup is shown in Fig. 1(a). Several reflections off a pair of negatively chirped mirrors compensate for the dispersion of the optical components, where fine tuning is achieved by tilting a fused silica window. The laser polarization is rotated by 45° using a half-wave plate, to provide both o and eo-polarized components for the nonlinear process.[9] A spherical mirror (focal length $f = 100$ mm) focuses the visible beam to a spot size of 30 μm on the $LiIO_3$ crystal. The emitted THz radiation is collimated with a BaF_2 lens and refocused onto a liquid-N_2 cooled HgCdTe detector, with remaining visible beam components blocked with a Ge window.

Spectra of the broadband THz pulses are obtained from interferometric field correlations.[8] As illustrated in Fig. 1(a), two visible beams are focused on the $LiIO_3$ crystal for this purpose. This generates two independent THz beams, which overlap due to divergence and interfere on the detector. An interferogram, as shown in Fig. 1(b), results from scanning the time delay Δt between the two visible pulses. The THz spectrum is then obtained from the Fourier transform of the interferogram.

As shown in Fig. 2(a), we observe generation of ultrabroadband THz pulses with the 113-μm crystal near normal incidence. The spectrum extends more than an octave from $\approx$ 40-90 THz. In contrast, Fig. 2(b) shows the spectrum obtained with a 1-mm thick $LiIO_3$ crystal, which by comparison exhibits a much narrower bandwidth. About 1 μW of THz power is generated from the thin crystal for 160 mW of incident visible power, as estimated from the calibrated detector sensitivity.

To elucidate the ultrabroadband phase-matching process in $LiIO_3$, we simulate difference frequency mixing of ultrashort pulses using the model of Ref. 10. Our calculation takes into account the dispersion of $LiIO_3$,[16] the measured pump spectra shown in Fig. 3(a), and the THz transmission of our crystal displayed in Fig. 3(b). Results are shown in Fig. 3(c)-(e) for two different combinations of the pump source and the internal phase-matching angle θ: pulses from the 9-fs oscillator with $\theta = 19^\circ$ (solid lines), and amplified pulses from a hollow-fiber compressor with $\theta = 21.5^\circ$ (dashed lines) discussed further below. For simplicity, a flat pump-pulse spectral phase is employed. The calculated THz spectrum for the oscillator-based source is shown in Fig 3(c) (solid line) and confirms the ultra-broadband phase-matching condition. It closely follows the experiment as seen from the comparison in Fig. 2(a). The calculations also provide the full time-domain THz electric field $E_{THz}(t)$ shown in Fig. 3(e). It reveals a few-cycle THz transient, corresponding to only $\tau_{\mathrm{P}} \approx 19$ fs pulse width (FWHM) of the intensity envelope.

Phase-matching for the type-I process is governed by the wavevector mismatch $\Delta k(\nu_1, \Delta\nu, \theta) \equiv (2\pi/c) \times \{n_e(\nu_2, \theta)\nu_2 - n_o(\nu_1)\nu_1 - n_o(\Delta\nu)\Delta\nu\}$, which must be minimized. Here, n_o and n_e are the ordinary and extraordinary refractive indices of $LiIO_3$. A convenient measure of phase-matching is the coherence length $L_{\mathrm{C}} \equiv 2/\Delta k$. The shaded areas in Fig. 3(d) indicate visible and THz frequency pairs ν_1, $\Delta\nu$ where $\mathrm{L_C} > 100$ μm, i.e. where efficient phase-matching occurs in our crystal. The large extent of these regions underscores the potential of $LiIO_3$ for ultrabroadband frequency mixing. The THz bandwidth is thus optimized by matching the frequency-pair area in Fig. 3(d) to the pump spectrum. A second limitation of the interaction is the group velocity mismatch between o and eo-polarized visible pulse components. Calculations show that while this mismatch vanishes for $\Delta\nu \approx 60$ THz, it can approach 100 fs/mm at higher frequencies. These aspects, along with broadening of the sub-10 fs visible pulses, contribute to the choice of ≈ 100 μm as an ideal crystal thickness for ultrabroadband THz generation.

With higher pulse energy and bandwidth, these THz pulses may also act as a broadband seed for phase-preserving chirped-pulse optical parametric amplifiers,[18] extending comparable schemes around 2 μm wavelength[19,20] towards the mid-IR. Such arguments, in turn, motivate the use of even shorter and more intense visible driving pulses. In a second experiment, we employ 7-fs pulses generated with a commercial 1-kHz multi-pass Ti:sapphire amplifier coupled to a hollow-fiber and chirped mirror compressor (HFC).[17] With the fiber filled with Ne at 1.7 bar, the pulse spectrum extends from 600–900 nm [dashed line, Fig. 3(a)]. A train of 200 μJ pulses with 7 mm $1/e^2$ beam diameter is transmitted unfocused through the 113-μm thick $LiIO_3$ crystal. We observe generation of THz radiation, characterized with a grating-based spectrometer.

Figure 4 shows the resulting extremely broadband THz spectrum (circles), which extends

from 50 to beyond 130 THz. A model calculation is shown for $\theta = 21.5°$ for an unchirped pump pulse (dashed line) and for -6 fs^2 quadratic chirp (solid line). The latter ensures optimal THz generation around 90 THz and mimics the experiment, where optimization occured by varying the insertion of thin fused silica wedges. Thus, excellent agreement between experiment and theory is achieved over most of the spectrum. Deviations below 50 THz are explained by long-wavelength limitations of our spectrometer. In Fig. 3(d), the coherence length area for $\theta = 21.5°$ is well adapted to the visible HFC spectrum. This clearly leads to a broadening and shift to higher frequencies. The calculated time-domain field in Fig. 3(e) predicts even shorter THz pulses with $\tau_P \approx 16$ fs. We measure a THz pulse energy of ≈ 8 nJ, corresponding to a quantum efficiency of 2×10^{-4}. This entails MV/cm field strengths when focused to a 100-μm spot size, with interesting perspectives for heterodyne mixing in high-harmonic generation or as streak fields in attosecond spectroscopy.[21]

In conclusion, we report the generation of ultrabroadband 50-130 THz pulses via phase-matched difference frequency mixing in $LiIO_3$. The usefulness of this compact scheme is demonstrated using different sub-10 fs pump sources. Model calculations give insight into the phasematching conditions, provide octave-spanning spectra that agree with experiment, and predict underlying few-cycle pulses with sub-20 fs duration.

We thank A. Cavalleri and R. W. Schoenlein for stimulating discussions, and Z. Hao and M.C. Martin for IR materials characterization. This study was sponsored by a MURI program of the Air Force Office of Scientific Research, grant FA9550-04-1-0242. Part of the work was supported by the U.S. Department of Energy, contract DE-AC02-05CH11231. R. H. and T.Z. acknowledge fellowships from the Alexander von Humboldt Foundation and German Academic Exchange Service, respectively.

*Present address, Department of Physics, University of Konstanz, 78464 Konstanz, Germany.

References

1. S. Woutersen, U. Emmerichs, and H. J. Bakker, Science **278**, 658 (1997).
2. R. A. Kaindl, *et al.*, Science **287**, 470 (2000).
3. R. Huber, *et al.*, Nature **414**, 286 (2001), ibid. Phys. Rev. Lett. **94**, 027401 (2005).
4. C. W. Luo, *et al.*, Phys. Rev. Lett. **92**, 047402 (2004).
5. T. Kampfrath, *et al.*, Phys. Rev. Lett. **95**, 187403 (2005).
6. G. Cerullo, S. De Silvestri, Rev. Sci. Instr. **74**, 1 (2003).
7. A. Bonvalet, M. Joffre, J.-L. Martin, and A. Migus, Appl. Phys. Lett. **67**, 2907 (1995).
8. M. Joffre, A. Bonvalet, A. Migus, and J.-L. Martin, Opt. Lett. **21**, 964 (1996).
9. R. A. Kaindl, *et al.*, Opt. Lett. **23**, 861 (1998).

10. R. A. Kaindl, F. Eickemeyer, M. Woerner, and T. Elsaesser, Appl. Phys. Lett. **75**, 1060 (1999).
11. R. Huber, A. Brodschelm, F. Tauser, and A. Leitenstorfer, Appl. Phys. Lett. **76**, 3191 (2000).
12. T. Fuji, A. Apolonski, and F. Krausz, Opt. Lett. **29**, 632 (2004).
13. M. Zimmermann, C. Gohle, R. Holzwarth, T. Udem, and T. W. Hänsch, Opt. Lett. **29**, 310 (2004).
14. K. Liu *et al.*, Appl. Phys. Lett. **85**, 863 (2004).
15. C. Kübler *et al.*, Appl. Phys. Lett. **85**, 3360 (2004).
16. M. M. Choy and R. L. Byer, Phys. Rev. B**14**, 1693 (1976).
17. S. Sartania, *et al.*, Opt. Lett. **22**, 1562 (1997).
18. C. P. Hauri, *et al.*, Opt. Lett. **29**, 1369 (2004).
19. T. Fuji, *et al.*, Opt. Lett. **31**, 1103 (2006).
20. C. Manzoni, *et al.*, Opt. Lett. **31**, 963 (2006).
21. T. Pfeifer, L. Gallman, M. Abel, P. Nagel, D. Neumark, and S. R. Leone, Phys. Rev. Lett., to appear (2006).

List of Figures

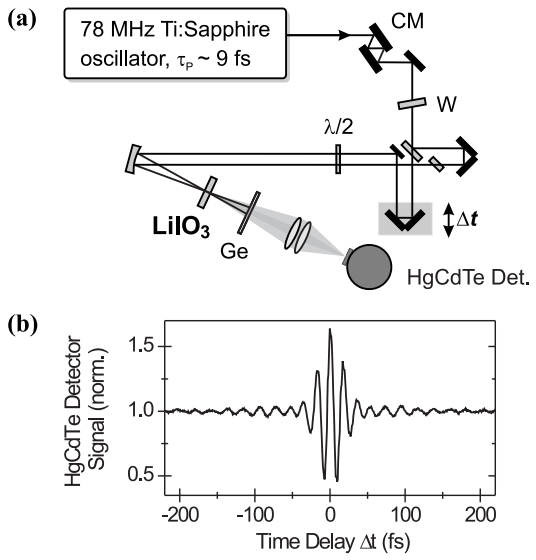

Fig. 1. (a) Oscillator-based setup for THz pulse generation in $LiIO_3$ and for interferometric field correlations. W: 1-mm thick fused-silica window, CM: chirped mirrors with ≈ -200 fs^2 group delay dispersion, Ge: Germanium window. (b) interferogram generated with a 113-μm thick crystal near normal incidence.

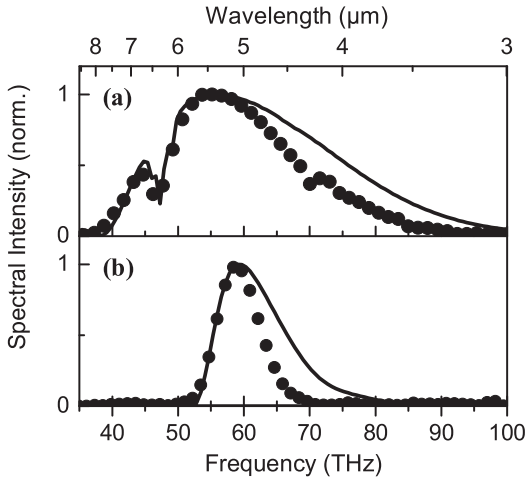

Fig. 2. Spectra of THz pulses generated in $LiIO_3$ with a 9-fs Ti:sapphire oscillator: (a) measured spectrum from a 113-μm thick crystal (dots) and model curve (line) at $\theta = 19°$. (b) as above, but for a 1-mm thick crystal and $\theta = 19.3°$.

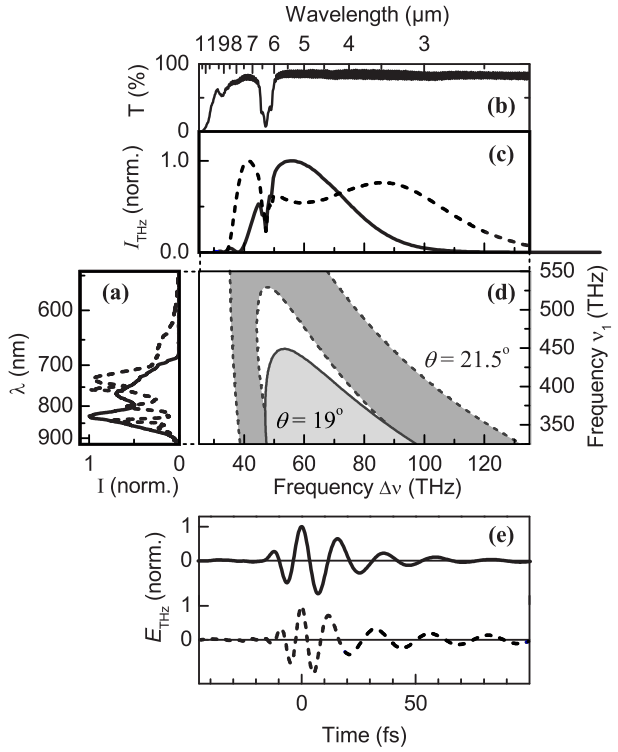

Fig. 3. (a) Spectra of 9-fs Ti:sapphire oscillator pulses (solid line) and of 7-fs pulses from a hollow fiber compressor, HFC (dashed). (b) normal incidence transmission of 113-μm thick $LiIO_3$. (c)-(e) Calculations of phase-matched difference frequency mixing in this crystal. Results are for $\theta = 19°$ pumped by the oscillator (solid lines), and for $\theta = 21.5°$ pumped by the HFC (dashed): (c) THz spectra, (d) frequency space (shaded) with $L_C > 100$ μm, (e) time-domain THz electric fields.

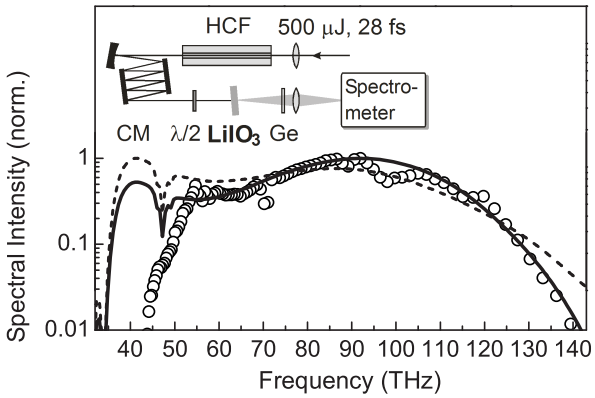

Fig. 4. Octave-spanning THz spectrum (circles) generated in $LiIO_3$ with 7-fs pulses from a hollow fiber compressor (inset). Model curves with $\theta = 21.5°$ are shown for unchirped pump pulses (dashed line) as in Fig. 3, and for -6 fs^2 quadratic chirp (solid line).